

INFLUENCE OF INVESTMENT CASTING MANUFACTURING CONDITIONS ON AS-CAST MICROSTRUCTURE AND EROSIWE WEAR RESISTANCE OF 26%Cr CAST IRON

Huynh Kinh Luan Ngo

Technical Division, Itoh Kikoh Co. Ltd., Tokai, Aichi 476-0001, Japan

Kaoru Yamamoto and Tetsuya Okuyama

Department of Materials System Engineering, National Institute of Technology, Kurume College, Kurume, Fukuoka 830-8555, Japan

Copyright © 2024 American Foundry Society
<https://doi.org/10.1007/s40962-024-01298-5>

Abstract

The relationship between the as-cast microstructure and erosive wear resistance of 26%Cr cast iron manufactured by investment casting was investigated in this study. Four samples were prepared by using two different shell mold temperatures and two different pouring temperatures. The delayed onset of solidification due to high shell mold temperature is more remarkable than that due to high pouring temperature. In two samples of hot-molds, it was found that the slower cooling rate results in coarsening of primary carbide cells and the formation of bainite in

matrix. A relative comparison of erosive wear resistance among four samples revealed that bainite accelerates the wear rate under severe erosive wear conditions. Little effect of fine carbides on the erosive wear resistance was found.

Keywords: investment casting, 26%Cr cast iron, as-cast microstructure, erosive wear resistance

Introduction

High Cr cast irons containing 26–30%Cr have excellent erosive wear resistance, so they are widely used for liner, blades and distributors, which are internal parts for shot blasting machines and surface treatment machines.^{1,2} Typical manufacturing casting processes for these products are known to be (1) self-hardening mold casting, (2) vacuum sealed molding process (V process casting) and (3) investment casting (lost-wax casting). Generally, when casting products with complex shape and wall thickness of 10mm or less than manufactured by self-hardening mold sand casting or V-process, misrun defects are likely to occur due to lower fluidity of molten. The defects also happen when the shell or the molten metal is too cold or the pouring rate is too slow. In contrast, it has been reported that the investment casting can suppress the occurrence of misrun defects.³

The shells (molds) used in the investment casting process are first modeled using a wax pattern material that is given a primary coating and then subsequent coatings of mullite and zircon-based refractory material developing the ceramic molds. These dry ceramic molds are transferred to an autoclave, where the wax patterns are melted in a hot steam environment. Subsequently, the investment shell is subjected to firing at the temperature of about 1000 °C. Generally, in the investment manufacturing process of cast steel and cast iron products, the molten metal is poured into hot-molds, of which the surface is red-hot after being removed from the firing furnace. In recent years, regarding the technology of investment casting, there have been many reports on the casting simulation of the investment casting and the development of its molding systems.^{4–7} Regarding cast steels and cast irons, most studies have been conducted using sand molds rather than ceramic molds because the preparation of ceramic molds in investment casting is complicated. It was reported that the slower cooling rate after casting causes the delayed onset of solidification, changing the microstructure and mechanical properties of some materials.^{8,9}

Kaoru Yamamoto and Tetsuya Okuyama have contributed equally to this work.

Received: 24 September 2023 / Accepted: 14 February 2024

Published online: 25 March 2024

In the case of high Cr cast irons, some of castings may be commercially used in either as-cast state or they may be heat-treated prior to use. Hence, there are numerous studies on microstructures in as-cast state, after destabilization treatment and their abrasive wear, erosive wear, corrosive wear resistance under various test conditions.^{10–16} It was reported that the wear behavior of high Cr cast irons varied with several factors: microstructure (metallic matrix, carbide) and wear test conditions. However, there are few reports of high Cr cast irons produced by investment casting compared to other casting processes. For example, it is still unclear whether the manufacturing conditions of investment casting affect the as-cast microstructure as well as the wear resistance of high Cr cast iron.

In the present study, four kinds of 26%Cr cast iron manufactured by investment casting at two pouring temperatures and two mold temperatures were subjected to an erosive wear test to clarify the relationship between as-cast microstructure and wear resistance. The wear behavior was also discussed.

Experimental Procedure

Sample Preparation

The test pieces used in this study were blades of 60 mm wide × 115 mm long × 11 mm thick. The wax patterns of blades were used to prepare ceramic shells. To preserve the fine details of the mold, the first layer on the wax surface (primary coat) used zircon slurry and zircon sand sprinkling, and the second layer used zircon slurry and mullite sand sprinkling. The third to sixth layers of coating and sprinkling were prepared with mullite to fabricate ceramic shells. The thickness of the ceramic shells after molding is about 8 mm. The shell molds were then dewaxed by high-pressure steam at about 150 °C to melt out and drain the wax. In order to prevent deformation or rupture of the shell during pouring, these shell molds (hereinafter referred to as molds) were heated for 3.6ks in a firing furnace at 1000 °C. As described in Table 1, two kinds of molds for casting were prepared in this study. After removal from the firing furnace, red-hot molds with a temperature of around 800 °C, as measured by an infrared radiation thermometer, were described as Hot-molds. On the other hand, molds that were cooled to room temperature after heating were defined as Cold-molds.

As for the casting conditions, the raw materials were melted in a 100kg high-frequency electric melting furnace, and the melted iron was then poured into Cold-molds and Hot-molds at two pouring temperatures (hereafter, P.T.) of 1550 °C and 1500 °C. Table 2 shows the chemical compositions of cast irons used in the present study. After

Table 1. Manufacturing Conditions for Experimental Samples

No	Sample	Manufacturing condition
1	Low P.T.— Cold mold	The mold of test pieces removed from the firing furnace were cooled to room temperature. Melted iron was poured at 1500 °C into cold molds
2	High P.T.— Cold mold	The molds of test pieces removed from the firing furnace were cooled to room temperature. Melted iron was poured at 1550 °C into cold molds
3	Low P.T.— Hot mold	The molds of test pieces immediately after being removed from the firing furnace have a temperature of about 800 °C into hot molds
4	High P.T.— Hot mold	The molds of test pieces immediately after being removed from the firing furnace have a temperature of about 800 °C into hot molds

Table 2. Chemical Compositions of Experimental Cast Iron (mass%)

C	Si	Mn	P	S	Ni	Cr	Mo	Fe
3.15	0.31	0.69	0.036	0.008	0.33	26.35	0.09	bal.

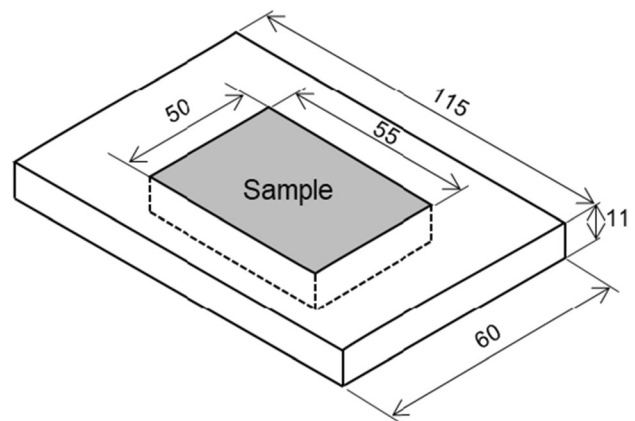


Figure 1. Shape of sample for erosive wear test.

casting, all samples were cooled naturally to room temperature in the molds. Based on such manufacturing conditions of blades, it is considered that the cooling rate after casting decreases in the order from No.1 (Low P. T.—Cold mold) to No.4 (High P. T.—Hot mold). As displayed in Figure 1, a rectangular sample with a width of 50 mm and a length of 55 mm cut from the center of each as-cast blade was subjected to the erosive wear test.

Evaluation of Erosive Wear Resistance

The erosive wear resistance was evaluated using a direct pressure abrasive blast machine (hereafter, wear test).^{1,12,15} After attaching the sample to the test table in the chamber of the testing machine, the distance from the nozzle tip with a diameter of 6mm to the sample was adjusted to 100 mm. Iron grit with a hardness of 850 HV and an average diameter of 1.2 mm was used as the abrasive media in the wear test. For each cycle of the wear test, 25 kg of iron grit was accelerated from the nozzle tip at a pressure of 0.5 MPa and impacted to the sample surface at normal angle. The samples were subjected to 21 cycles of wear test, and the testing time of each cycle was about 1.0 ks. Unlike the erosive wear test conditions in most relevant references, it was observed that under the present wear test conditions, many sparks were generated from the surface sample due to the impact of iron grit. According to Miyasaka et al.,¹⁷ the average of iron grit was above 100m/s from a nozzle tip to sample surface. Therefore, wear of the material under such severe erosive wear conditions is also referred to as “impact wear.”

After every three cycles of testing, weight loss and thickness reduction in each sample were measured using an analytical electronic balance and a contact profilometer, respectively. Additionally, the sample surface was photographed after 6, 12, 18, 20 and 21 cycles.

Microstructural Characterization

Samples for microstructural observation were wet polished with SiC emery paper and buffed with alumina suspension, followed by etching in Vilella's reagent (HCl: 5 ml, picric acid: 1 g, ethanol: 100 ml) for 7–10 seconds. The microstructures of all as-cast samples were investigated using an optical microscope (OM, Keyence VHX—2000) and a scanning electron microscope (SEM, JEOL IT—100LA). As for SEM observation, the secondary electron (SE) was used, which provides a proper contrast between phases. After the wear test, the worn surfaces were also observed in both SE and backscattered electron (BE) modes.

Phase identification was carried out using an X-ray diffractometer (XRD, Empyrean by Malvern PANalytical, Cu-K α) in the range of 2θ from 30 to 60°. Amount of retained austenite was measured by an X-ray diffraction method using a special goniometer with automatic rotating and swinging sample stage. The X-ray beam was Mo-K α characteristic line with Zr filter. The scanning range of 2θ was from 24 to 44°. The amount of austenite was calculated from the ratio of peak areas of (200) and (220) for ferrite or martensite, and those of (220) and (311) for austenite.

Hardness Measurement

Hardness on the sample surface was measured using a Vickers hardness tester (Akashi, AVK-A). The average hardness of each sample was taken from ten measurements at a load of 196 N (20 kgf). Also, measurement of hardness distribution from surface in the depth direction of as-cast sample was occurred at the same load. After the wear tests, a micro Vickers hardness tester (Shimadzu, HMV-G21 FA) was used to measure at a load of 2.94 N (0.3 kgf) for assessment of work hardening of each sample. The load holding time for each measurement was 15 s for both hardness testers. The average hardness of each sample was taken from five measurements.

Measurement of Bainitic and Martensitic Transformation Start Temperature

Thermal analysis was performed using a thermomechanical analyzer (TMA, Rigaku Thermo plus EVO2). For each manufacturing condition, a cylindrical sample with a diameter of 5 mm and a height of 15 mm was cut from the blade by wire cutting. In the TMA test, the samples were heated in an argon atmosphere to 1000 °C and cooled to room temperature at a cooling rate of 5 and 50°C/min without holding at that temperature. As for the bainitic and martensitic transformations, a tangent line was drawn on the straight portion of cooling curve just before expansion appeared in the curve, and the points at which the cooling curve was apart from the tangent line were adopted as the start of transformations.

Results and Discussion

As-Cast Microstructure

The microstructures of the surface and cross section of each sample were observed to investigate whether the manufacturing conditions of blades affected the as-cast microstructure. First, the sample surfaces of all blades were slightly polished by about 0.1 mm with wet SiC emery paper. By etching in Vilella's reagent, it can be visually seen that flower petal-like patterns appeared from the polished surface. From Figure 2 showing the low-magnification OM images, it was seen that these patterns varied depending on the manufacturing conditions. The petal patterns were smaller and denser in two samples of Cold-molds compared to Hot-molds. In addition, at the same pouring temperature, the number of petal patterns reduced but their size became coarser with increasing the shell mold temperature. From the high magnification OM images shown in the same figure, it was recognized that each petal pattern is an aggregate of primary carbides. As indicated by the white dotted line, each eutectic carbide cells filled the space between primary carbides. Difference in morphology

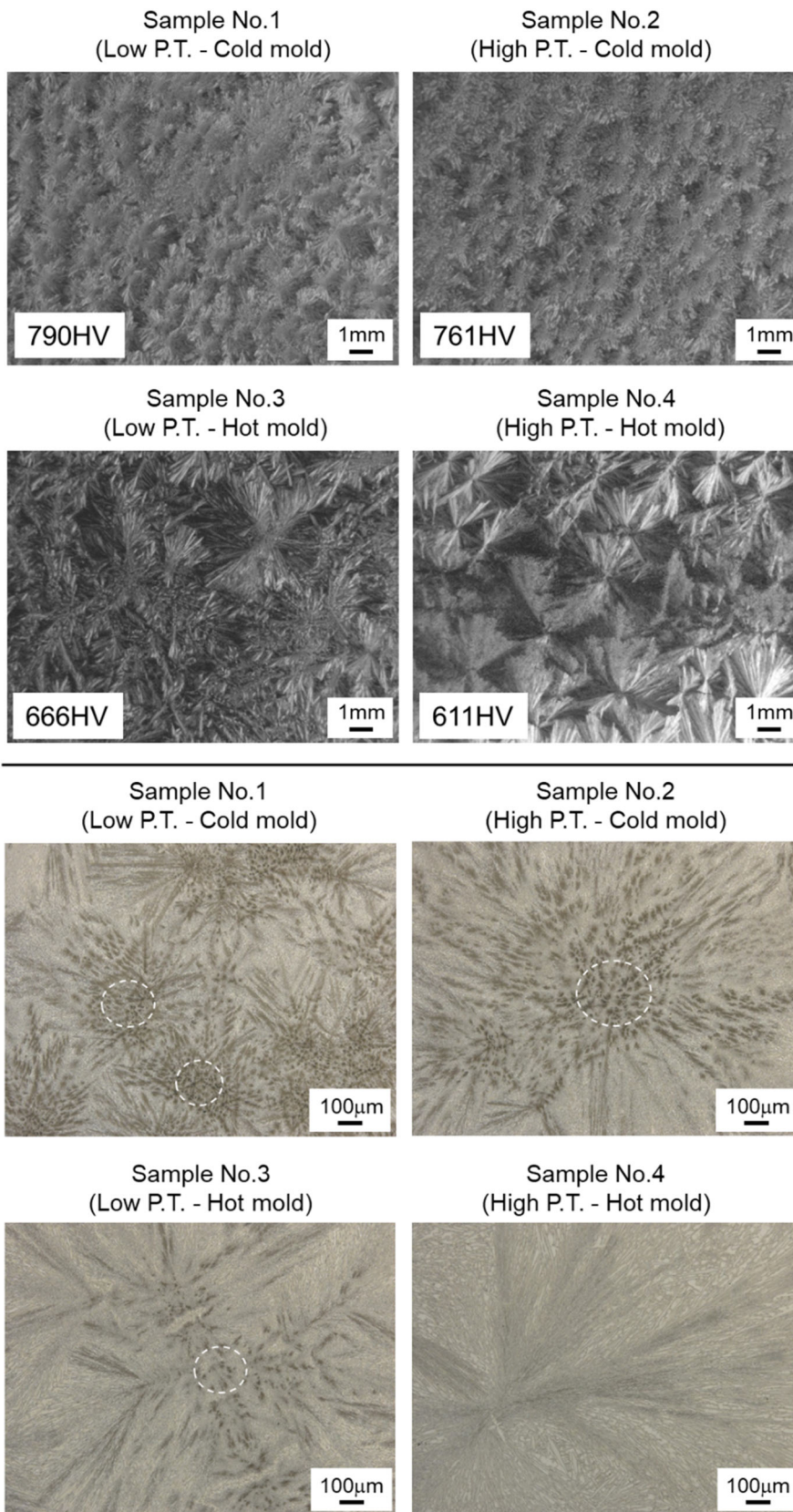


Figure 2. Optical microscopy (OM) images showing microstructures of sample surfaces in as-cast state.

of primary carbides due to cooling rate was observed from vertical direction not only in the experimental cast iron (eutectic structure) but also in hypereutectic cast iron. Primary carbides of high Cr cast iron are known to be type M_7C_3 , always rod-shaped, with hexagonal in cross section. Subsequent solidification around the primary carbides results in the formation of finer blade-like carbide. As the cooling rate is slower, the blade-like carbide shape is favored.^{18,19} In this study, it is considered that the difficult heat release to the sample wall for Hot-molds, causing the primary carbide to coarsen easily.

As displayed in the low magnification OM images, it was also found that there was a difference in the hardness measured at the surface of the four samples. The average hardness measured on the surface decreases in the following order: Low P.T.—Cold mold, Low P.T.—Hot mold, High P.T.—Cold mold, High P. T.—Hot mold.

Figure 3 displays the cross-sectional microstructure near-surface of each sample. Unlike samples of Cold-molds, it was observed that the sub-surface layer appeared in samples of Hot-mold which was due to the continuous growth of primary carbides. The sub-surface layer, which is mainly the aggregate of primary carbides, has a thickness of 30–50 μm for sample No.3 (Low P.T.—Hot mold) and 140–160 μm for sample No.4 (High P.T.—Hot mold). Meanwhile, the surface layer in two samples of Cold-molds was negligible, being only a few μm . As mentioned above, when heat release to the sample wall for Hot-molds becomes difficult, the primary carbides easily coarsen. As a result, from cross-sectional direction (lateral direction), the

sub-surface layer was formed due to growth of primary carbides. Comparison of sub-surface layer revealed that effect of shell mold temperature on the microstructure near surface is more pronounced than that of pouring temperature. Therefore, it can be stated that the formation and growth of primary carbides in both samples of Hot-molds is one of the characteristics of high Cr cast irons with a eutectic structure manufactured by investment casting process.

Figure 4 shows the cross-sectional microstructures at the center of each sample observed by SEM at high magnification. For the samples of Cold-molds, it was observed that mainly primary carbides were embedded in the matrix. In contrast, some fine carbide regions in the matrix surrounded by primary carbides were detected in samples of Hot-molds, as indicated by black arrows, which are not found in the samples of Cold-molds. Moreover, the number of fine carbide regions tends to increase with increasing pouring temperature for Hot-molds. From these results, it was determined that changes in manufacturing conditions caused differences in the microstructure at the surface as well as at the center.

The results of phase identification by XRD for the sample surface and cross section are shown in Figure 5. From the XRD pattern results of the sample surfaces, it is clear that the main primary Cr carbide present on the surface was M_7C_3 . Additionally, the peak intensity of martensite is higher than that of austenite for samples of Cold-molds (No. 1 and No. 2). Conversely, the peak intensity of austenite is relatively higher for the samples of Hot-molds

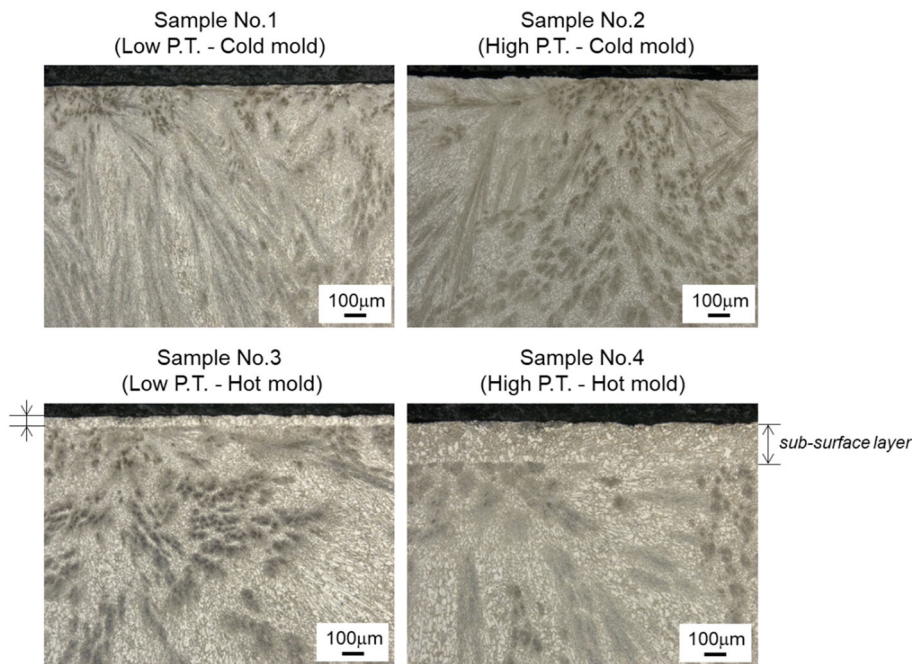


Figure 3. Optical microscopy (OM) images showing cross-sectional microstructures adjacent to sample surfaces.

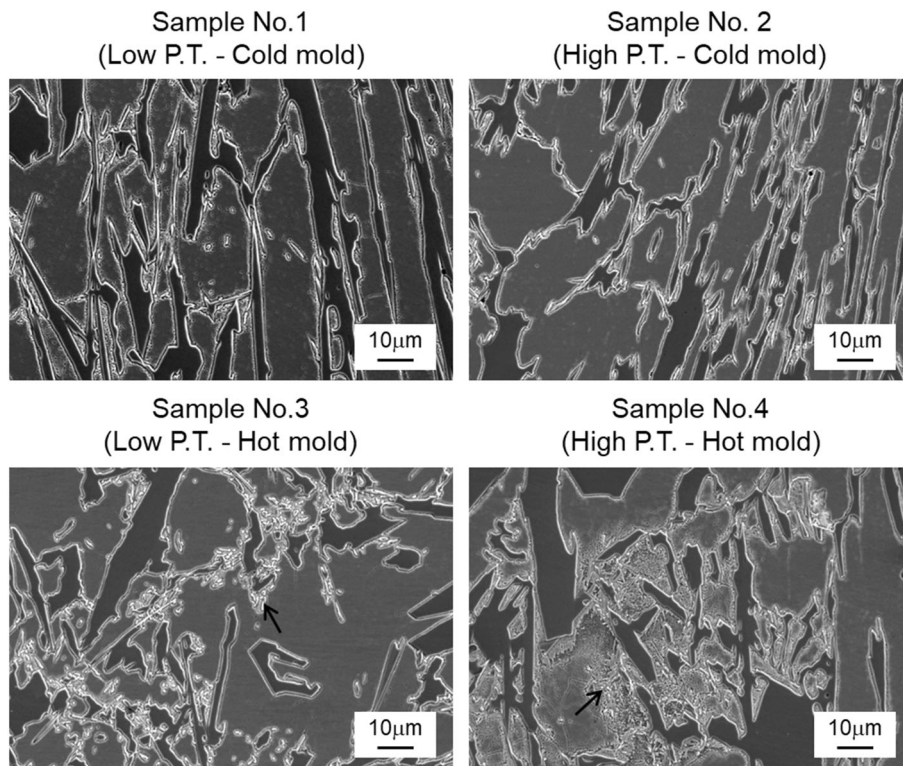


Figure 4. Scanning Electron Microscopy (SEM) images showing the difference in cross-sectional microstructure near center of samples.

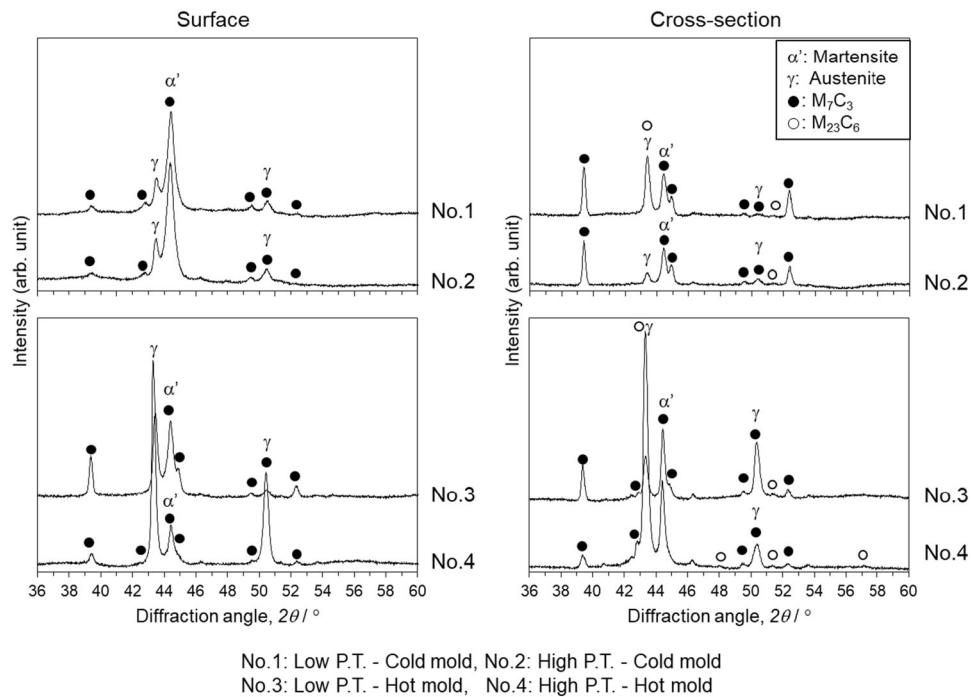


Figure 5. XRD results of surface and cross section of samples in as-cast state.

(No. 3 and No. 4). At the same mold, it was observed that the peak intensity of martensite decreased. In contrast, the peak intensity of austenite increased at higher pouring temperatures. Therefore, at higher mold and pouring temperatures, slower cooling rates are presumed to stabilize

austenite near the surface. On the other hand, it was also found that the results of the cross section were similar to the surface when comparing the peak intensity ratio of martensite and austenite in all samples. However, besides M_7C_3 , it was detected the appearance of $M_{23}C_6$ in the

matrix for two samples of Hot-molds, unlike Cold-molds. Consequently, fine carbides surrounded by primary carbides indicated by the black arrows in Figure 4 are presumed to be $M_{23}C_6$.

Figure 6 displays the amount of retained austenite at the surface and at a depth of 5.5 mm from surface (the center of sample) measured by XRD. It can be recognized that in any sample, the amount of retained austenite at the surface is lower than that at surface, indicating that austenite is relatively stable at the center as compared to the surface. Furthermore, the stability of austenite at the surface varied depending on the manufacturing conditions. In detail, the austenite amount at the surface increases in the following orders: Low P.T.—Cold mold, Low P.T.—Hot mold, High P.T.—Cold mold, High P. T.—Hot mold. At the center of every sample, the austenite amount was approximately 60%.

Microstructures of 25%Cr cast iron manufactured by the self-hardening sand mold casting were investigated at various cooling rates after casting by Tamura et al.¹¹. When the demolding sample after casting above is slower, the obtained matrix was mainly bainite and / or pearlite, and hardness was relatively low. To confirm whether bainitic or pearlitic transformation occurs during cooling after solidification for the experimental cast iron, thermal analysis by TMA was performed for all samples. Figure 7 shows the displacement curves after reaching 1000 °C and cooling to room temperature at two different cooling rates without holding the temperature. At a 50 °C/min cooling rate, the martensitic transformation started at the same temperature of 260 °C for two samples of Cold-molds, regardless of pouring temperature. In contrast, the martensitic and bainitic transformations were recognized to occur in both samples of Hot-molds. The bainitic start temperature (Bs) and the martensitic temperature (Ms) were 335 °C and 265 °C, respectively. As the cooling rate

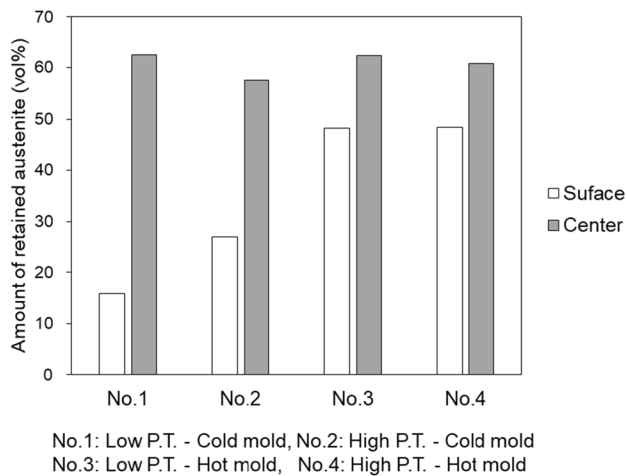


Figure 6. Amount of retained austenite at surface and center of samples in as-cast state.

of TMA decreased by 5 °C/min, it was seen that Bs shifted to 40 °C higher and two-stage transformation of martensite (Ms_1 and Ms_2) appeared in the hot mold samples. At the same cooling rate, Ms_1 and Ms_2 were also observed in samples Cold-molds, but no bainitic transformation was detected. The two-stage transformation of martensite can be explained by solute C in matrix. A cooling rate of 50 °C/min in TMA test, the diffusion time of the alloying elements is very short. Therefore, alloying elements were difficult to diffuse due to normal segregation. In contrast, the cooling rate is relatively slow, the elements can diffuse during cooling stage. Since the alloying elements, especially solute carbon were taken up by the crystallized carbides, the concentration of alloying elements in the vicinity of the carbides decreases. As a result, the bainitic transformation and/or martensitic transformation occurs around the carbides. Ms_1 and Ms_2 appear at a cooling rate of 5 °C/min in TMA test was due to the segregation of solute C and the other alloying elements remaining in austenite around primary carbides. Similarly, the appearance of bainite in the sample of Hot-molds was a results of decrement of solute carbon near carbides, because fine carbides of $M_{23}C_6$ around primary carbides of M_7C_3 in the samples of Hot-molds easily precipitate during cooling after solidification.

From the above results, it can be stated the as-cast microstructures of experimental cast iron manufactured by investment casting was heterogeneous. Not only carbide but also the amount of metallic phase in matrix change from the surface to center. The difference in as-cast microstructure was caused by the difference in cooling rate after casting among four samples.

Figure 8 shows the hardness distribution in the thickness direction for all samples. The maximum hardness near the surface sample varied depending on the manufacturing conditions. The hardness for two samples of Cold-molds is higher than that of Hot-molds. Furthermore, a decrease in hardness from the surface to a depth of 1.5 mm was observed regardless of manufacturing conditions. When the depth exceeded 1.5 mm from the surface, the hardness for any sample was almost constant. The results of hardness distribution correspond well to the microstructural changes from surface to center.

Erosive Wear Test Results

Figure 9 displays photographs of the sample surfaces that changed during the wear test. After test cycle of 6, it was visually confirmed that some uneven patterns had formed on the surface of the two samples of Hot-molds, while the damage of surfaces due to wear was little on the two samples of Cold-molds. As the number of test cycles increases, the wear region spreads from the sample center and further develops in the depth direction, forming a

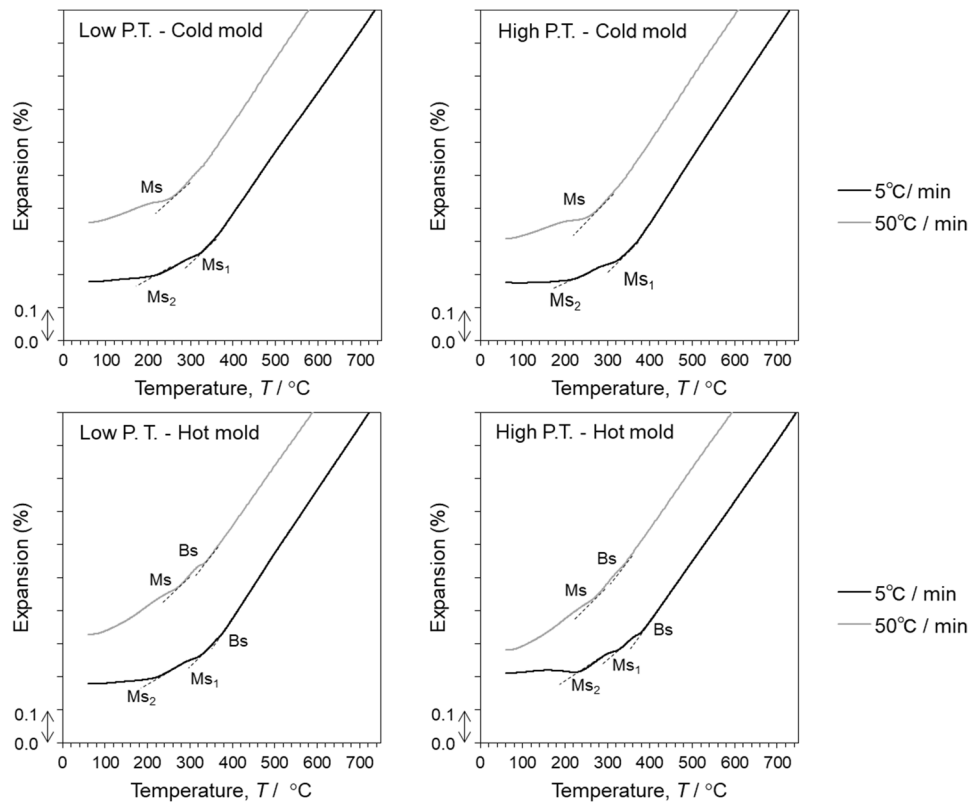


Figure 7. Dilatometry curves for experimental samples during cooling.

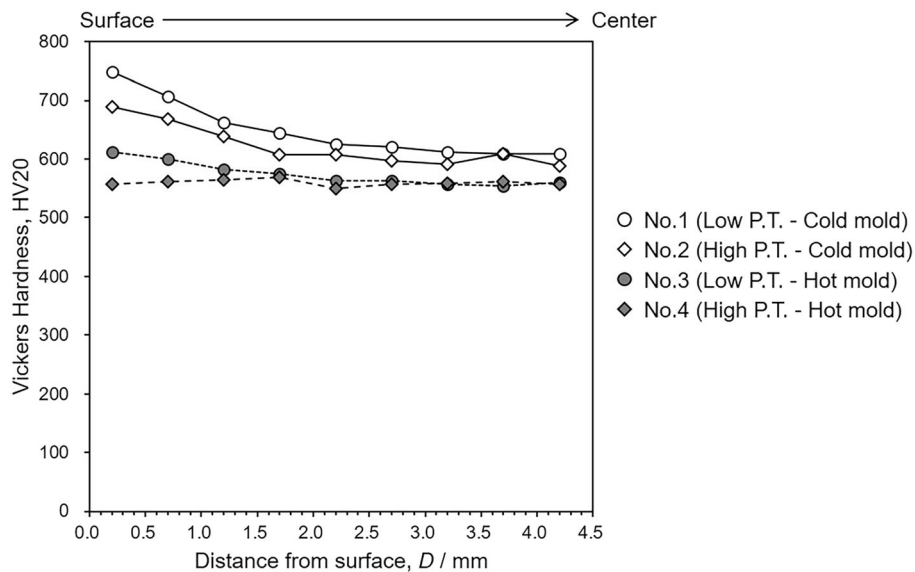


Figure 8. Hardness profiles of samples from surface to center.

crater. The diameter and depth of the crater for sample No.4 are observed to be the largest among them. After the wear tests were completed, the uneven patterns around the crater remained intact in two samples of Hot-molds. In contrast, some wavy patterns were observed in two samples of Cold-molds. From these appearances, it could be concluded that pouring the melted iron in the hot mold at a higher pouring temperature is unfavorable because a

slower cooling rate after casting would cause the degradation of erosive wear resistance. Lowering the pouring temperature of the melted iron before casting could reduce the wear rate. As for both samples of Cold-molds, excellent wear resistance was exhibited. In other words, the cooling rate after casting plays an important role in the erosive wear resistance of experimental cast iron in as-cast state.

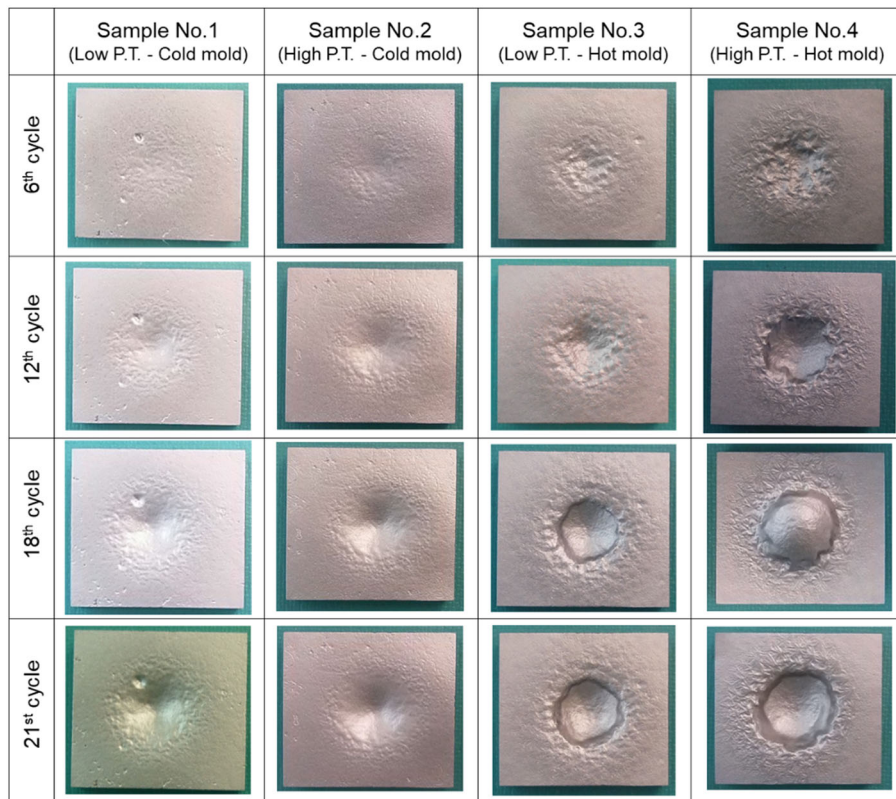


Figure 9. Appearance of sample surfaces during erosive wear tests.

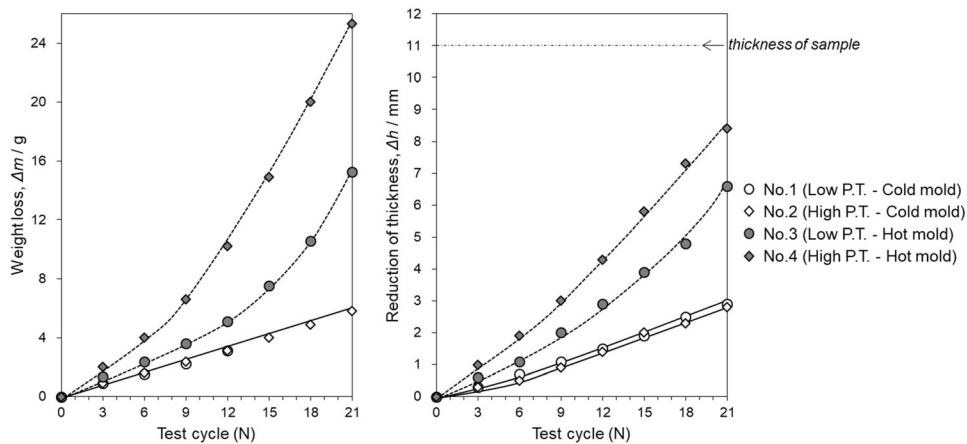


Figure 10. Change in weight loss and thickness reduction in samples during erosive wear tests.

The relationship between the weight loss and thickness reduction in each sample and the test cycle number is shown in Figure 10. It was seen that the weight loss for sample No.1 and sample No.2 (Cold-mold) linearly increases with increasing the test cycles. The reduction in thickness gradually increases up to the first 6 cycles and then increases linearly in the depth direction. It was difficult to recognize the difference in wear rate between two samples of Cold-molds caused by the pouring temperature. However, it is worth noting that increasing the pouring

temperature remarkably increases not only the weight loss but also the thickness reduction when poured into two samples of Hot-molds. After the wear test was completed, sample No. 4 had the largest weight loss, followed by sample No. 3. Weight loss of sample No.2 was almost the same as sample No.1. Regarding the reduction in thickness, it was found that wear exceeded the sample thickness by more than half in sample No. 3 and sample No. 4, but only by one third in sample No. 1 and sample No. 2. These results emphasized that the erosive wear resistance of high

Cr cast irons manufactured by investment casting process varies with the shell mold temperature and the pouring temperature.

Conventionally, pouring molten iron into the ceramic mold immediately after removal from the firing furnace is known to be a standard condition for investment casting; however, the as-cast products do not exhibit a desirable erosive wear resistance. It is recommended to set austenitizing temperature above 1050 °C¹² to ensure erosive wear resistance of castings prior to use.

After the erosive wear tests, the hardness profiles in the depth direction from the most worn surface of all samples were shown in Figure 11. Each measured value indicates the harness of a mixture of matrix and Cr carbides. From the figure, it was obvious that a significant hardening of the surface occurs due to the blasting of iron grit. Focusing on the relatively large work-hardening region at a distance of 30 μm from the surface, the maximum hardness of sample No.1 exceeds 1000HV, while that of sample No.4 is 880HV, which is much lower.

Here, we try to evaluate the degree of work hardening after wear test. Since not only the change in microstructure from surface to center but also the hardness profile of all samples (Figure 8) indicated that as-cast microstructures of four kinds of high Cr cast iron manufactured by investment casting was heterogeneous, the degree of work hardening (ΔHV) of all samples in the present study is defined as the following equation:

$$\Delta HV = HV_{\text{max at surface after wear test}} - HV_{\text{initial at the same depth}}$$

where $HV_{\text{max after wear test}}$: Maximum hardness below the worn surface after wear test, HV_{initial} : Hardness of the as-cast sample measured at the same depth to the worn sample, respectively.

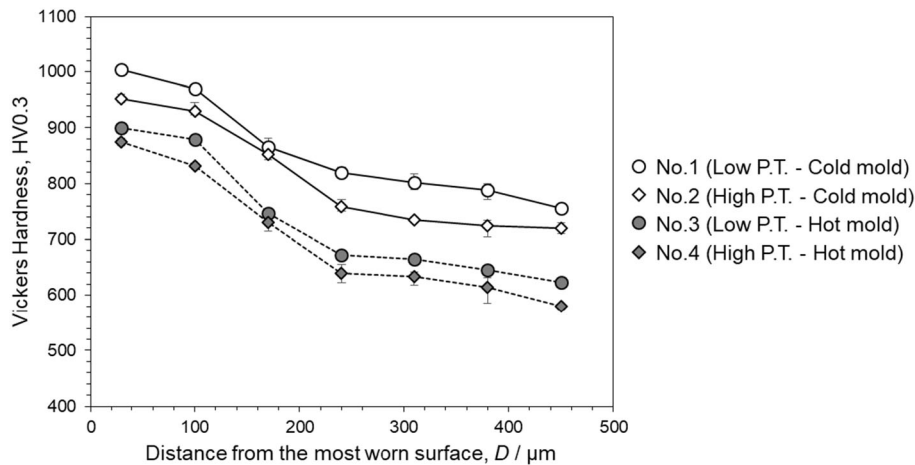
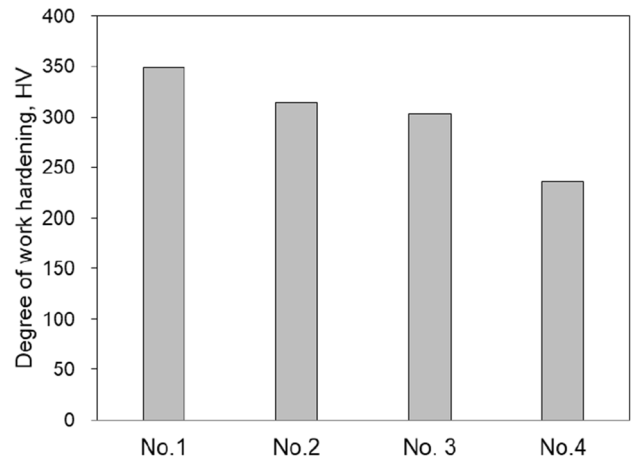


Figure 11. Hardness profiles below the most worn surface after erosive wear tests.

From Figure 12, difference in erosive wear rate may be explained in terms of the degree of work hardening. The higher the ΔHV , the slower the wear rate. The lower the ΔHV , the faster the wear rate. This means that the maximum hardness near the surface reflects the erosive wear resistance. Previous studies have shown that only metastable retained austenite, rather than martensite, plays an important role in improving erosive wear resistance.¹⁵ Under erosive wear test condition in the present study, the martensitic transformation from metastable austenite occurred due to impingement of iron grit to sample surface.

Microstructure After Wear Test

Sample No.1 (Low P. T.—Cold mold) and sample No.4 (High P. T.—Hot mold) were selected to investigate



No.1: Low P.T. - Cold mold, No.2: High P.T. - Cold mold
No.3: Low P.T. - Hot mold, No.4: High P.T. - Hot mold

Figure 12. Degree of work hardening amount below the most worn surface.

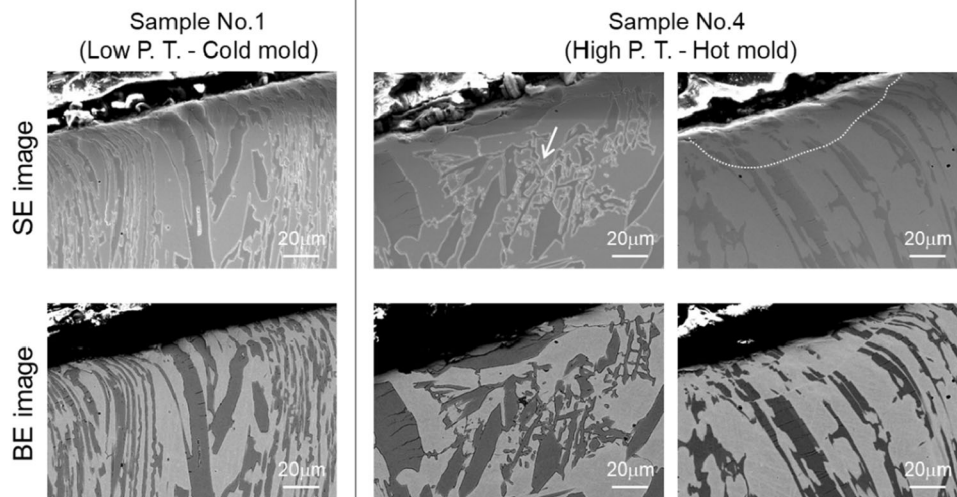


Figure 13. Cross-sectional microstructures beneath the most worn surfaces for sample No.1 (Low P.T.—Cold mold) and sample No.4 (High P. T.—Hot mold) after erosive wear tests.

whether there were differences in microstructure beneath the most worn surface. The representative SE and BE images of cross-sectional microstructures are displayed in Figure 13. Cracking of primary carbides was observed in both samples. In sample No.1, the primary carbides with the same growth direction were densely distributed in a hard matrix, making it difficult for the fractured carbides to detach from surface. However, the SEM observation of sample No. 4 revealed that some debris of carbide remained in these coarse non-directional primary carbides before detachment, while there was no debris for fine carbides. As mentioned earlier, the contribution of bainite to work hardening is relatively small compared to metastable austenite. Under the continuous impingement of iron grit, it is considered that the fractured carbides were easy to detach from the matrix near surface. Additionally, as indicated by the dotted line, some of the fractured primary carbides are shifted laterally, giving the appearance of being cut. Such deformation tended to occur significantly in the samples of Hot-mold, regardless of pouring temperature. From the obtained results, it can be concluded that the wear behavior of 26%Cr cast iron produced by investment casting depends on the as-cast microstructure as cast.

Relationship Between As-Cast Microstructure and Erosive Wear Resistance of High Cr Cast Iron

In order to clarify the influence of cooling rate after casting on as-cast microstructure and wear resistance, the wear test result of 27%Cr cast iron manufacturing by sand mold casting^{12,15} in the previous study was compared with the wear test result of experimental cast iron after test cycle of 20. It is known that use of a metal chiller can suppress the occurrence of shrinkage cavity in the complex shape

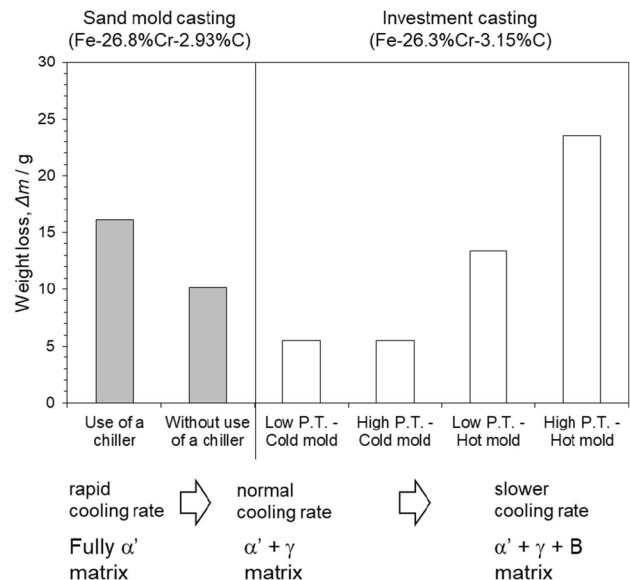


Figure 14. Comparison of erosive wear resistance of high Cr cast irons manufactured by investment casting and sand mold casting after test cycle of 20. The data of sand mold casting were extracted from the previous study.¹²

castings. In previous study, effectiveness of a metal chiller was confirmed to 27%Cr cast iron manufactured by sand mold casting. The as-cast microstructure of 27%Cr cast iron where attached the metal chiller consisted of a predominant martensitic (α') matrix with fine primary carbides due to the relatively fast cooling rate. In contrast, the area without use of the metal chiller solidified at the normal cooling rate, so the obtained matrix was a mixed structure of retained austenite (γ) and martensite. From Figure 14, it was seen that a predominant martensitic matrix exhibited a significantly larger weight loss as compared to a mixed

structure of retained austenite and martensite in matrix. In the present study, a relative comparison of four samples solidified with four different cooling rates revealed that the slower cooling rate resulted in the formation of bainite (B) in the matrix and increased weight loss. The results indicate the effect of metallic matrix is more significant as compared to carbides, so the cooling rate after casting in each casting process is a very important factor that cannot be ignored.

It was reported that the microstructure of 24–27%Cr cast irons after destabilization treatment at lower temperature consisted of a predominant martensitic matrix with dense and fine secondary carbides, whereas higher austenitizing temperature resulted in the matrix of predominant metastable austenite with limited secondary carbides.¹⁰ Regardless the use of a chiller or not, destabilization treatment at the austenitizing at 950 °C deteriorated the erosive wear resistance of high Cr cast irons. In contrast, destabilization treatment at temperatures of 1150 °C can improve the erosive wear resistance. Regarding the investment casting, in the case of castings with large wall thickness and complex shape, lowering the temperature of mold may cause the crack of mold during pouring the molten. For assurance of the erosive wear resistance, the high Cr cast irons products should be heat-treated at the high austenitizing temperature before use.

Conclusions

The influences of pouring temperature and shell mold temperature in the investment casting process on the as-cast microstructure and erosive wear resistance of 26%Cr cast iron were investigated. The obtained findings were as follows:

1. Pouring molten iron into the red-hot mold causes the discontinuous growth of primary carbides near-surface. From the depth direction, a thin layer of coarsened carbides is observed near the surface of the Hot-mold samples, which is not found in the Cold-mold samples. Also, under the manufacturing condition, bainite and fine carbides form in the matrix at the center of sample.
2. The erosive wear resistance of high Cr cast iron varies with the investment casting manufacturing conditions such as pouring temperature and shell mold temperature.
3. Metastable retained austenite is effective in improving the erosive wear resistance, whereas only martensite or the presence of bainite in matrix are not desired since they accelerate the wear rate. Effect of fine carbides on the erosive wear resistance was smaller than that of coarse carbides.

REFERENCES

1. H.K.L. Ngo, K. Koizumi, K. Mizuno, Y. Yamada, T. Okuyama, Influence of as-cast microstructure on the impact wear resistance of 27 mass%Cr cast iron. *Mater. Trans.* **60**, 2475–2480 (2019). <https://doi.org/10.2320/matertrans.F-M2019844>
2. M. Agustina Guitar, U. Pranav Nayak, Dominik-Britz and Frank-Mücklich: the effect of thermal processing and chemical composition on secondary carbide precipitation and hardness in high-chromium cast irons. *Int. Metalcast.* **14**, 755–765 (2020). <https://doi.org/10.1007/s40962-020-00407-4>
3. K. Matsuno, Feature of investment casting. *IMONO* **66**, 681–687 (1994)
4. S. Pattnaik, D.B. Karunakar, P.K. Jha, Developments in investment casting process—a review. *J. Mater. Process. Technol.* **212**, 2332–2348 (2012). <https://doi.org/10.1016/j.jmatprotec.2012.06.003>
5. M. Xu, S.N. Lekakh, V.L. Richards, Thermal property database for investment casting shells. *Int. Metalcast.* **10**, 329–337 (2016). <https://doi.org/10.1007/s40962-016-0052-4>
6. H. Inoue, Technical review of precision casting from Latest Literature. *JFS* **69**, 783–794 (1997). <https://doi.org/10.11279/jfes.69.783>
7. Kumar, D.B. Karunakar, Characterization and properties of ceramic shells in investment casting process. *Int. Metalcast.* **15**, 98–107 (2021). <https://doi.org/10.1007/s40962-020-00421-6>
8. R. Singh, S. Singh, Effect of process parameters on surface hardness, dimensional accuracy and surface roughness of investment cast components. *J. Mech. Sci. Technol.* **27**, 191–197 (2013). <https://doi.org/10.1007/s12206-012-1218-5>
9. H. Huang, P. Fu, Y. Wang, L. Peng, H. Jiang, Effect of pouring and mold temperatures on hot tearing susceptibility of AZ91D and Mg–3Nd–0.2Zn–Zr Mg alloys. *Trans. Nonferrous Met. Soc. China* **24**, 922–929 (2014). [https://doi.org/10.1016/S1003-6326\(14\)63144-7](https://doi.org/10.1016/S1003-6326(14)63144-7)
10. C.L. Nue, S.C. Gallo, A. Vahid, J. Wang, M. Taherishargh, H. Attar, D. Fabijanac, M. Barnett, Destabilization treatment and its influence on microstructure and matrix hardness of high-Cr cast iron. *Metall. Mater. Trans. A* **54**, 4952–4965 (2023). <https://doi.org/10.1007/s11661-023-07216-4>
11. A. Tamura, S. Nitta, H. Ono, Control of microstructure and abrasion resistance of 25 mass % Cr cast irons. *IMONO* **66**, 187–192 (1994). https://doi.org/10.11279/imono.66.3_187
12. H.K.L. Ngo, K. Koizumi, K. Mizuno, Y. Narita, Y. Yamada, T. Okuyama, Influence of quenching temperature on impact-wear resistance of 27%Cr cast iron. *J. JFS* **93**, 11–19 (2021). <https://doi.org/10.11279/jfes.93.11>
13. X.H. Tang, R. Chung, D.Y. Li, B. Hinckley, K. Dolman, Variations in microstructure of high

- chromium cast irons and resultant changes in resistance to wear, corrosion and corrosive wear. *Wear* **267**, 116–121 (2009). <https://doi.org/10.1016/j.wear.2008.11.025>
14. B.M. Rajcic, A. Maslarevic, G.M. Bakic, V. Maksimovic, M.B. Djukic, Erosion wear behavior of high chromium cast irons. *Trans. Indian Inst. Met.* **76**(2023), 1427–1437 (2023). <https://doi.org/10.1007/s12666-022-02860-7>
 15. H.K.L. Ngo, K. Koizumi, K. Mizuno, K. Mizuno, Y. Yamada, T. Okuyama, M. Nakayama, Role of matrix structure on impact-wear resistance of As-quenched 27%Cr cast iron. *Mater. Trans.* **63**, 740–747 (2022). <https://doi.org/10.2320/matertrans.F-M2022803>
 16. V. Heino, M. Kallio, V. Valtonen, V.-T. Kuokkila, The role of microstructure in high stress abrasion of white cast irons. *Wear* **388–389**, 119–125 (2007). <https://doi.org/10.1016/j.wear.2017.04.029>
 17. Miyasaka, Surface improvement technology “wonder process craft (WPC)” by rapid impact of fine particle. *J. Vac. Soc. Jpn.* **51**, 30–34 (2008). <https://doi.org/10.3131/jvsj2.51.30>
 18. R. Reda, A. Nofal, K. Ibrahim, A. Hussien, Investigation of improving wear performance of hypereutectic 15%Cr–2%Mo white Irons. *China Foundry* **7**, 438–446 (2011)
 19. A. Nofal, R. Reda, K. Ibrahim, A. Hussien, Structural refinement of 15%Cr–2%Mo white irons. *Key Eng. Mater.* **457**, 231–235 (2011). <https://doi.org/10.4028/www.scientific.net/KEM.457.231>

Publisher’s Note Springer Nature remains neutral with regard to jurisdictional claims in published maps and institutional affiliations.

Springer Nature or its licensor (e.g. a society or other partner) holds exclusive rights to this article under a publishing agreement with the author(s) or other rightsholder(s); author self-archiving of the accepted manuscript version of this article is solely governed by the terms of such publishing agreement and applicable law.